

Research



Cite this article: Tagliabue A, Resing J. 2016
Impact of hydrothermalism on the ocean iron
cycle. *Phil. Trans. R. Soc. A* **374**: 20150291.
<http://dx.doi.org/10.1098/rsta.2015.0291>

Accepted: 13 July 2016

One contribution of 20 to a discussion meeting
issue 'Biological and climatic impacts of ocean
trace element chemistry'.

Subject Areas:
oceanography

Keywords:
hydrothermalism, ocean biogeochemistry,
ocean iron cycle, ocean carbon cycle,
ocean ventilation

Author for correspondence:
Alessandro Tagliabue
e-mail: a.tagliabue@liverpool.ac.uk

Impact of hydrothermalism on the ocean iron cycle

Alessandro Tagliabue¹ and Joseph Resing²

¹School of Environmental Sciences, University of Liverpool,
Liverpool, UK

²Joint Institute for the Study of the Atmosphere and Ocean,
NOAA-PMEL and the University of Washington, Seattle,
WA 98115, USA

AT, 0000-0002-3572-3634

As the iron supplied from hydrothermalism is ultimately ventilated in the iron-limited Southern Ocean, it plays an important role in the ocean biological carbon pump. We deploy a set of focused sensitivity experiments with a state of the art global model of the ocean to examine the processes that regulate the lifetime of hydrothermal iron and the role of different ridge systems in governing the hydrothermal impact on the Southern Ocean biological carbon pump. Using GEOTRACES section data, we find that stabilization of hydrothermal iron is important in some, but not all regions. The impact on the Southern Ocean biological carbon pump is dominated by poorly explored southern ridge systems, highlighting the need for future exploration in this region. We find inter-basin differences in the isopycnal layer onto which hydrothermal Fe is supplied between the Atlantic and Pacific basins, which when combined with the inter-basin contrasts in oxidation kinetics suggests a muted influence of Atlantic ridges on the Southern Ocean biological carbon pump. Ultimately, we present a range of processes, operating at distinct scales, that must be better constrained to improve our understanding of how hydrothermalism affects the ocean cycling of iron and carbon.

This article is part of the themed issue 'Biological and climatic impacts of ocean trace element chemistry'.

1. Introduction

Via the process known as the biological pump, carbon fixation by marine phytoplankton and subsequent

sinking of organic carbon to depth are able to affect the global carbon cycle and atmospheric CO₂ concentrations [1]. As such, variations in the availability of the resources that regulate phytoplankton growth and the sinking (or export) of organic carbon will have important ramifications for the carbon cycle. An area of particular focus in this regard is the Southern Ocean, where due to the formation of deep water, modifications to the biological pump have a particularly strong impact on atmospheric CO₂ [2]. Until the mid-1980s, our conceptual view of resource limitation in the ocean focused on nitrogen and phosphorus, but at this time the emergence of new contamination-free measurement methods emphasized an important role for the trace metal iron (Fe) [3–5]. Following a spate of *in situ* experiments, the central role of iron in regulating phytoplankton activity and the biological pump in the Southern Ocean is now well established [6–8].

A focus of research in the ocean iron cycle has been the evaluation of the strength of different iron sources. Until relatively recently, the only significant source of Fe to the open ocean was considered to be the deposition of Fe-rich mineral dust [9]. Accordingly, variations in the dust supply of iron during the geologic past are often invoked as drivers of the glacial–interglacial changes in atmospheric CO₂ [10]. However, recent findings are challenging this paradigm and pointing to the importance of other sources in regulating the global ocean iron cycle. One such source is that associated with deep-sea hydrothermal vents where the interaction between seawater and rock at elevated temperatures and pressures produces hydrothermal fluids with greatly elevated Fe concentrations [11]. These hot Fe-rich fluids rise above the seafloor producing hydrothermal plumes with Fe concentrations hundreds of times greater than background values [12]. Despite this noted enrichment in Fe, our conceptual view of the impact of hydrothermalism on the iron cycle was that virtually all of this Fe was precipitated close to the vent sites, with little far field impact [9,13,14].

In the past 5–10 years, the progress made by the GEOTRACES programme (www.geotraces.org) has revolutionized our conceptual view of how hydrothermal vents affect the oceanic cycling of Fe. A discrete set of observations finding elevated Fe close to hydrothermal systems [15] or distal anomalies in Fe linked to the noted hydrothermal tracer ³He [16] provided initial indications of the importance of hydrothermal Fe. But it was the first large-scale GEOTRACES sections conducted as part of the international polar year that noted widespread Fe signals linked to noted hydrothermal sites in the Southern [17] and Arctic [18] Oceans. When a hydrothermal Fe source was added to an ocean biogeochemical model, it was found to have a large influence on interior-ocean Fe concentrations and improved the ability of the model to reproduce Fe observations [19]. Importantly, hydrothermally sourced Fe is ventilated primarily in the Southern Ocean and so has a direct impact on carbon export in this important region [19].

An important component of hydrothermal Fe supply concerns the residence time of hydrothermal Fe, which ultimately drives its ability to influence Southern Ocean carbon export. Follow-up work has confirmed distal Fe signals associated with hydrothermal systems in the Atlantic and Pacific Oceans, with effort focusing on constraining the gross global hydrothermal Fe flux [20–23]. A focused GEOTRACES section that crossed the mid-ocean ridge axis in the southeast Pacific demonstrated an unprecedented propagation of a hydrothermal Fe plume for more than 4000 km off-axis [24]. Importantly, this study noted quasi-conservative behaviour of dissolved Fe within the plume, indicating that it must be largely stabilized. When this process was accounted for in a global biogeochemical model, the impact of hydrothermal Fe on Southern Ocean carbon export doubled [24].

In this work, we take a state of the art ocean biogeochemistry model that accounts for the ocean iron cycle in a relatively complex manner to explore hypotheses regarding the influence of hydrothermal Fe on Southern Ocean carbon export. We assess the role of gross hydrothermal fluxes and Fe stabilization via a suite of GEOTRACES sections, quantify the relative role played by ridges in different ocean basins, the importance of gross Fe fluxes and Fe stabilization in the plume, and emphasize the need to place results in the context of ocean ventilation pathways to assess the ultimate impact on the Southern Ocean carbon cycle.

2. Methods

We conducted twelve 500-year simulations with the PISCES model [25] as described in Resing *et al.* [24] that are detailed in table 1. The first four experiments included a control experiment with the flux of hydrothermal Fe only (CTL), a 10-fold increase in hydrothermal Fe flux (CTL-10), no hydrothermal Fe flux (CTL-NOHYD) and an equimolar flux of iron and iron-binding ligands (CTL-L). We then conducted a set of experiments that aimed to examine the contribution of Fe from ridges in specific ocean basins. We conducted experiments where hydrothermal Fe flux came only from ridges south of 40°S, which we name ‘Southern ridges’ (SOC) and a parallel set of experiments where hydrothermal Fe flux came only from ridges north of 40°S. Under these scenarios, we then consider the specific contributions of ridges in the Atlantic (ATL), Pacific (PAC) and Indian (IND) ocean basins. This definition of the Southern ridges aims to isolate the contribution from the circum-Antarctic ridge system, but includes a small portion of the most southerly parts of Atlantic, Pacific and Indian ridges. These four simulations were then repeated with an equimolar ligand flux from hydrothermal supply (ATL-L, PAC-L, IND-L and SOC-L). We note here that while the response of the iron cycle is not linear, the mismatch between the total response and the sum of the individual ridge experiments amounts to 7% and 14% for the runs without and with ligand stabilization, respectively.

The PISCES model has a state of the art Fe cycle that is one of the best in capturing global trends from the latest Fe datasets [26]. PISCES has Fe sources from dust, sediments, rivers and hydrothermal vents and employs a dynamic model of ligand cycling that explicitly accounts for ligand sources and sinks [24,27]. The lifetime of iron-binding ligands is modelled via a ligand continuum with prescribed minimum and maximum lifetimes of 1 and 1000 years. As an example, when the ligand concentration is 2 nmol l⁻¹ the lifetime is 20 years, while at 0.4 nmol l⁻¹ the lifetime is increased to 450 years. Fe is lost via particle scavenging of free Fe, as well as colloidal pumping/aggregation with a variable colloidal Fe fraction [24]. Phytoplankton have a flexible requirement for Fe and Fe limitation of growth follows a quota model approach where the required demand varies in response to their growth environment [25].

3. Results

(a) Hydrothermal iron along the GEOTRACES transects

The GP-16 ran zonally from Ecuador to Tahiti in the southern sub-tropical Pacific (figure 1a), documenting a substantial hydrothermal plume that propagated westward for over 4000 km [24] (figure 1b). As discussed in [24], the model simulation that includes hydrothermal Fe only (figure 1c) is not able to capture the spatial extent of the observed Fe plume, even when hydrothermal inputs are increased 10-fold (figure 1d). A significantly long-lived hydrothermal iron plume is only generated by the simulation that includes equimolar fluxes of iron and stabilizing ligands (figure 1e). The model simulation that eliminates hydrothermal Fe input mostly fails to reproduce abyssal Fe distributions (figure 1f).

The GA-02 cruise was a meridional section running down the entire Atlantic basin (figure 2a). The section generated information on a number of Fe features, including a signal of a remote hydrothermal plume at around 2–3.5 km water depth centred on approximately 5°S [28] (figure 2b). Neither the hydrothermal Fe model simulation nor the simulation with 10-fold more hydrothermal Fe is able to reproduce this feature (figure 2c,d). Only the simulation that includes hydrothermal Fe stabilization is able to generate a broadly similar feature, albeit smaller in magnitude (figure 2e). The simulation without hydrothermal Fe emphasizes the hydrothermal origin of this feature (figure 2f).

The GA-03 cruise made a zonal transect across the North Atlantic sub-tropical gyre (figure 3a) and observed a hydrothermal signal from the Trans-Atlantic Geotraverse (TAG) site over the mid-Atlantic ridge (MAR) [20] (figure 3b). Simulations where only hydrothermal Fe is considered greatly underestimate this feature (figure 3c). However, when hydrothermal Fe is either increased

Table 1. A short description of the model experiments conducted in this study. All simulations were conducted for 500 years and are identical except for the specific differences described.

experiment name	experiment details
CTL	hydrothermal Fe active globally
CTL-L	as CTL but with equimolar supply of Fe ligands
CTL-10	as CTL, but 10× greater hydrothermal Fe supply globally
CTL-NOHYD	as CTL, but no hydrothermal Fe input globally
ATL	only Atlantic ridges north of 40° S supply hydrothermal Fe
PAC	only Pacific ridges north of 40° S supply hydrothermal Fe
IND	only Indian ridges north of 40° S supply hydrothermal Fe
SOC	only ridges south of 40° S supply hydrothermal Fe
ATL-L	as ATL but with equimolar supply of Fe ligands
PAC-L	as PAC but with equimolar supply of Fe ligands
IND-L	as IND but with equimolar supply of Fe ligands
SOC-L	as SOC but with equimolar supply of Fe ligands

10-fold, or added with stabilizing ligands the magnitude and lateral extent of the observed feature are reproduced reasonably well (figure 3*d,e*).

The CoFeMUG cruise, undertaken between Namibia and Brazil in the South Atlantic Ocean (figure 4*a*), observed a strong hydrothermal signal over the MAR [21] (figure 4*b*). As discussed in [21], a model simulation with only hydrothermal Fe is unable to reproduce this plume (figure 4*c*), while a 10-fold greater supply of Fe does a much better job (figure 4*d*). When hydrothermal iron stabilization is included the plume magnitude also increases in line with that observed but its lateral extent is largely overestimated (figure 4*e*).

(b) What is the impact of specific ridges to the Southern Ocean biological pump?

Our model includes hydrothermal Fe input from ridges in the Indian, Atlantic, Pacific and Southern ocean basins with a gross global hydrothermal input of 11.3 Gmol Fe yr⁻¹ [29]. The CTL, CTL-L and CTL-NOHYD simulations produce estimates of total Southern Ocean (south of 40° S) export production of 139, 142 and 146 Tmol C yr⁻¹, respectively, which compare well to data-based estimates that range from 70 to 260 Tmol yr⁻¹ [30–32]. By region, the Indian, Atlantic, Pacific and Southern ridges account for 9, 14, 41 and 35% of the total hydrothermal iron input, respectively (figure 5). If we separately consider each of these ridge systems as the sole source of hydrothermal Fe to the ocean, the relative impact on Southern Ocean export production is greatest from Pacific and Southern ridges (37 and 57%, respectively, figure 5) and is relatively low for the Atlantic and Indian ridges (2 and 12%, respectively, figure 5). When the simulations are repeated including hydrothermal Fe stabilization, the relative impact of Atlantic and Southern ridges increases to around 6 and 65%, respectively (figure 5), with a corresponding decline in the relative impact of Pacific and Indian ridges (to 32 and 11%, respectively, figure 5). In absolute terms the impact on carbon export in the Southern Ocean for the Indian, Atlantic, Pacific and Southern ridges is 4.0–8.0 × 10¹¹, 0.7–4.4 × 10¹¹, 12.8–22.6 × 10¹¹ and 19.5–45.9 × 10¹¹ mol C m⁻² yr⁻¹, respectively (the range accounts for simulations without and with a flux of stabilizing ligands; table 2).

Our results also demonstrate the relative response of carbon export in the three different geographical sectors of the Southern Ocean to hydrothermal input (with and without stabilization) from specific ridges (figure 6 and table 2). Pacific ridges have the largest carbon

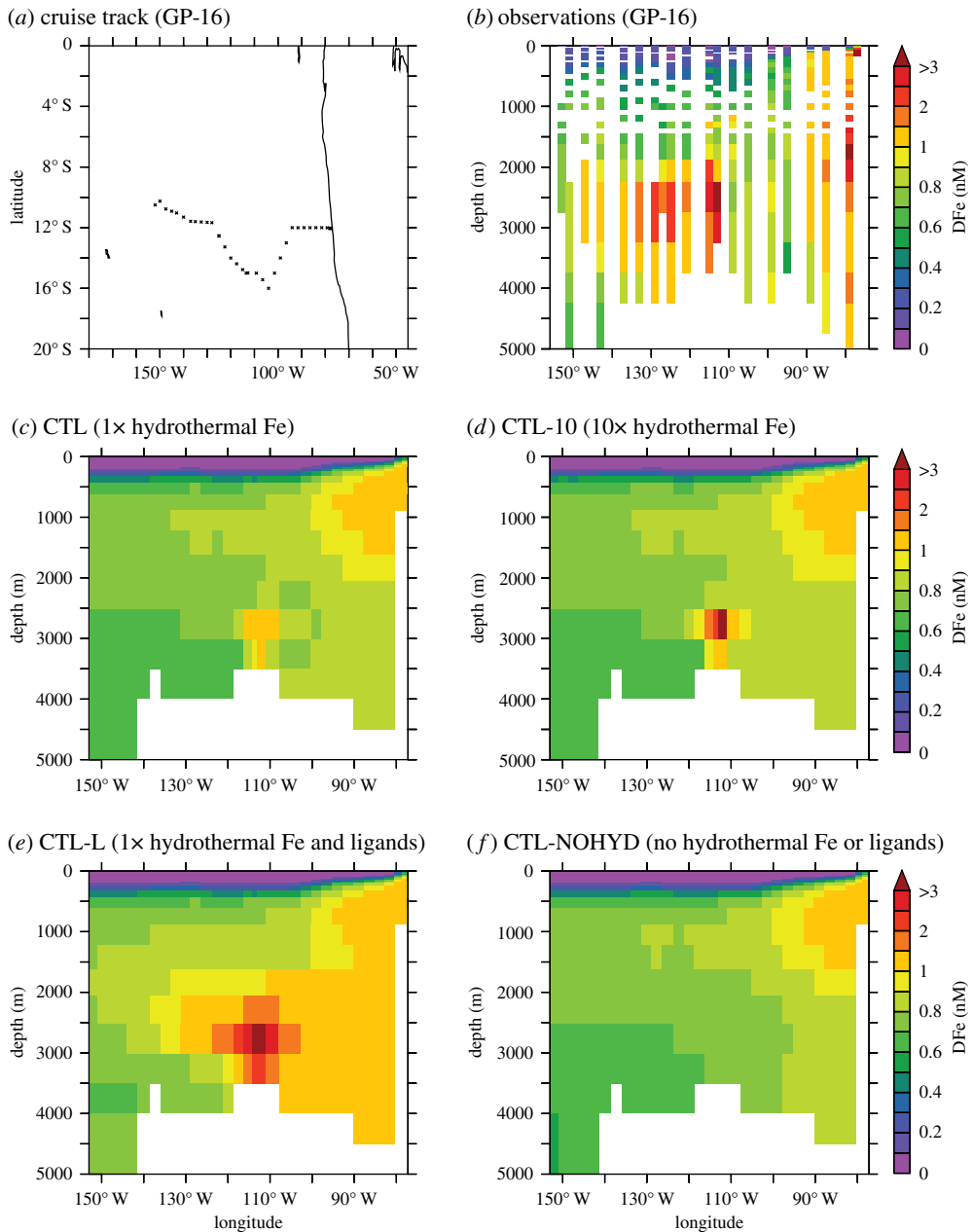


Figure 1. GP-16 (a) cruise track and (b) dissolved iron measurements, compared to model output from (c) CTL (hydrothermal iron supply only), (d) CTL-10 (10 times greater hydrothermal iron supply), (e) CTL-L (hydrothermal iron supply alongside an equimolar flux of iron-binding ligands) and (f) CTL-NOHYD (no hydrothermal iron supply).

export response in the Pacific sector of the Southern Ocean; however, their influence is also seen in the Atlantic and Indian sectors (figure 6). Indeed, the Atlantic sector of the Southern Ocean responds much more strongly to Pacific Ocean ridges ($2.6\text{--}5.9 \times 10^{11} \text{ mol C m}^{-2} \text{ yr}^{-1}$, without and with stabilization, respectively) than to Atlantic Ocean ridges ($0.2\text{--}1.1 \times 10^{11} \text{ mol C m}^{-2} \text{ yr}^{-1}$, without and with stabilization, respectively). Ridges in the Indian Ocean have a roughly equal impact on carbon export in both the Indian ($1.7\text{--}3.0 \times 10^{11} \text{ mol C m}^{-2} \text{ yr}^{-1}$, without and with stabilization, respectively) and Pacific ($1.6\text{--}3.0 \times 10^{11} \text{ mol C m}^{-2} \text{ yr}^{-1}$, without and with

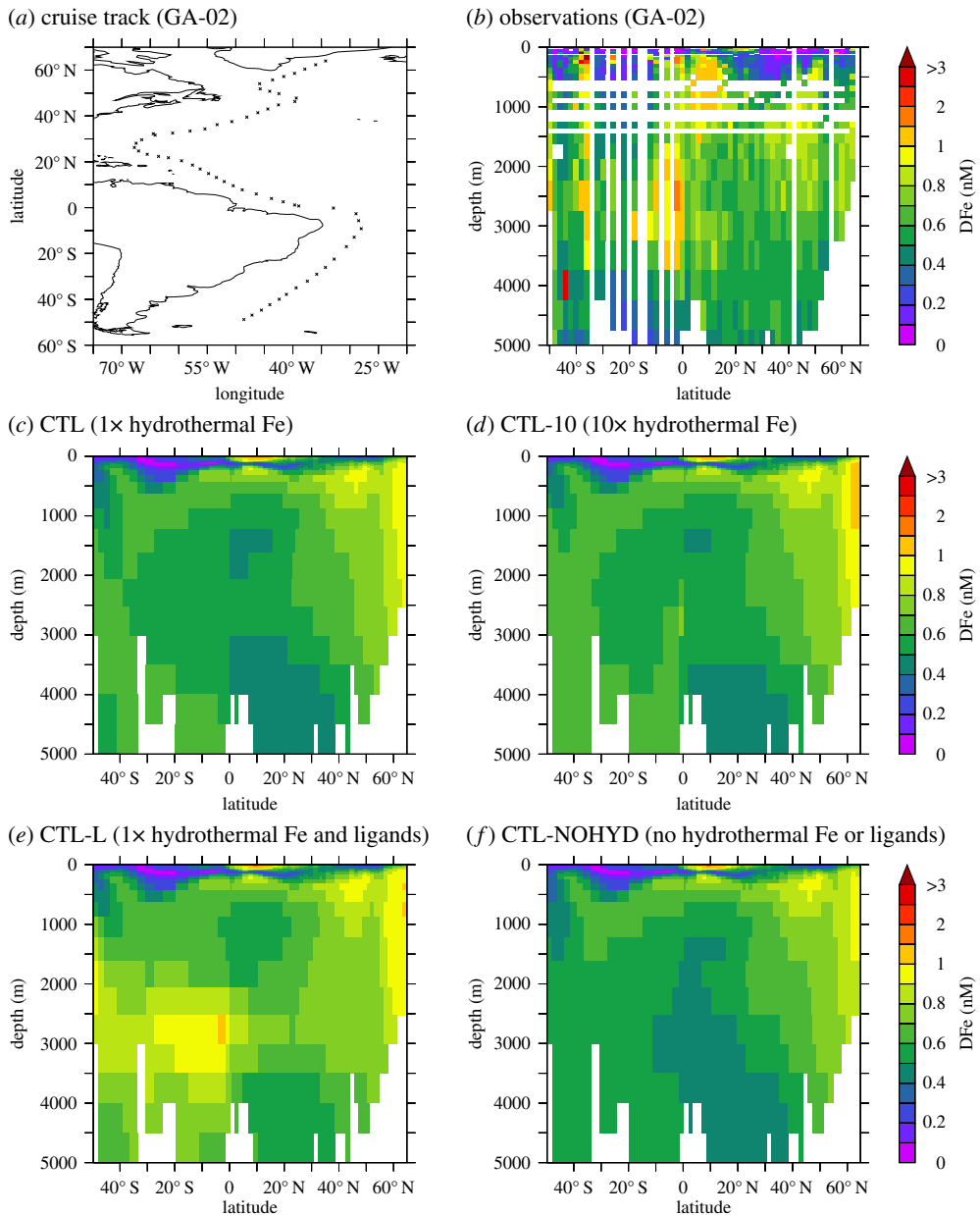


Figure 2. GA-02 (a) cruise track and (b) dissolved iron measurements, compared to model output from (c) CTL (hydrothermal iron supply only), (d) CTL-10 (10 times greater hydrothermal iron supply), (e) CTL-L (hydrothermal iron supply alongside an equimolar flux of iron-binding ligands) and (f) CTL-NOHYD (no hydrothermal iron supply).

stabilization, respectively) sectors of the Southern Ocean. Atlantic ridges have a muted influence throughout the Southern Ocean, when only Fe is considered; when stabilization is included their impact on other Southern Ocean basins increases. Finally, the largest response in absolute terms (apart from the Pacific sector) is found in response to Southern Ocean ridges (figure 6 and table 2), which increases greatly when stabilization is included and overwhelms the impact of distal sources in the Atlantic and Indian sectors. Overall, while stabilization changes the magnitude of the carbon export responses in each sector, the inter-sector patterns and trends are unaffected (figure 6).

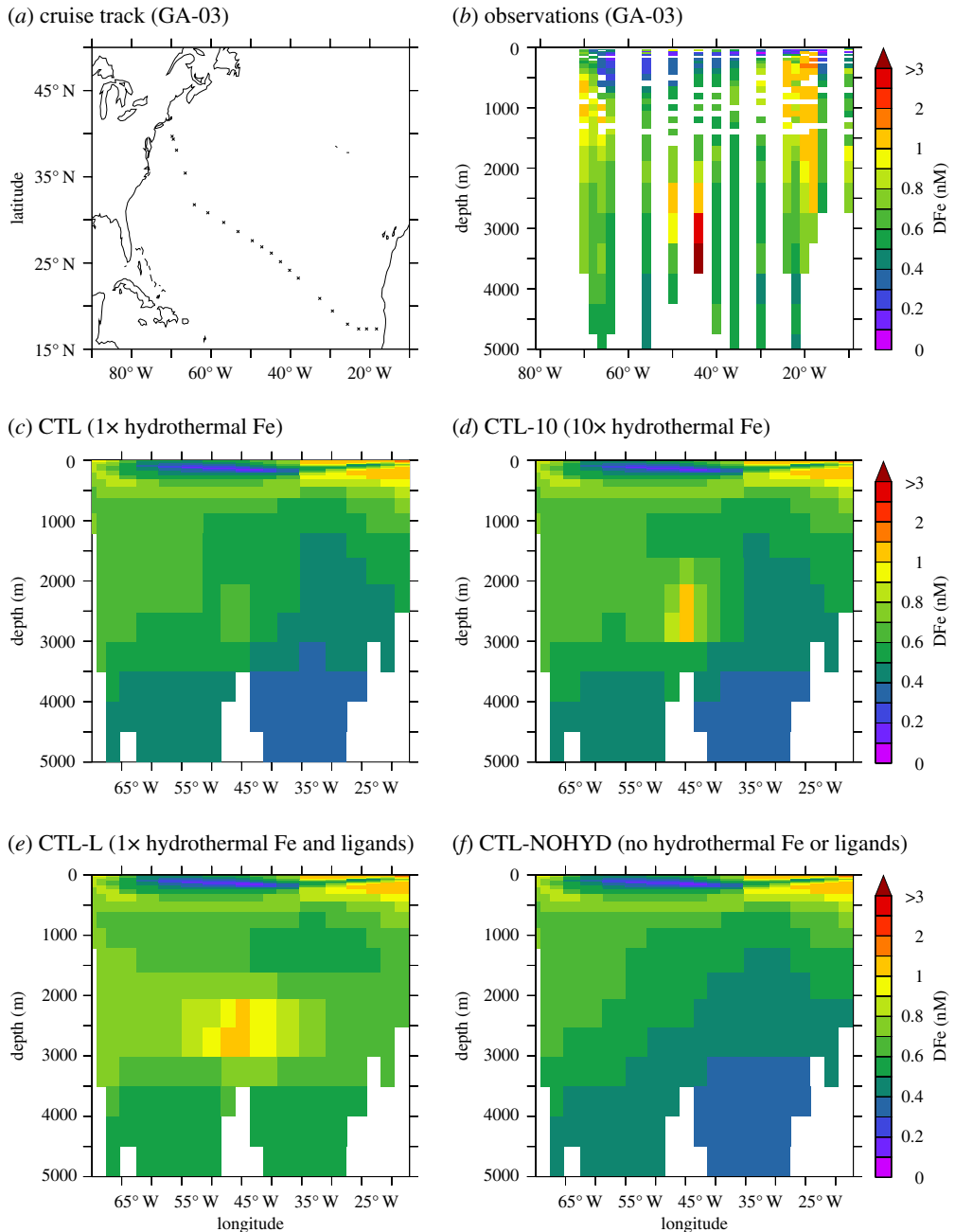


Figure 3. GA-03 (a) cruise track and (b) dissolved iron measurements, compared to model output from (c) CTL (hydrothermal iron supply only), (d) CTL-10 (10 times greater hydrothermal iron supply), (e) CTL-L (hydrothermal iron supply alongside an equimolar flux of iron-binding ligands) and (f) CTL-NOHYD (no hydrothermal iron supply).

(c) Importance of ventilation pathways

For hydrothermal Fe to stimulate carbon export in the Fe-limited Southern Ocean, it needs to be transported and ventilated at the surface. The ventilation pathways for hydrothermal Fe can be investigated by examining the density surface at which hydrothermal Fe is supplied and the eventual outcrop region for this isopycnal layer in the Southern Ocean. In general, we find broad

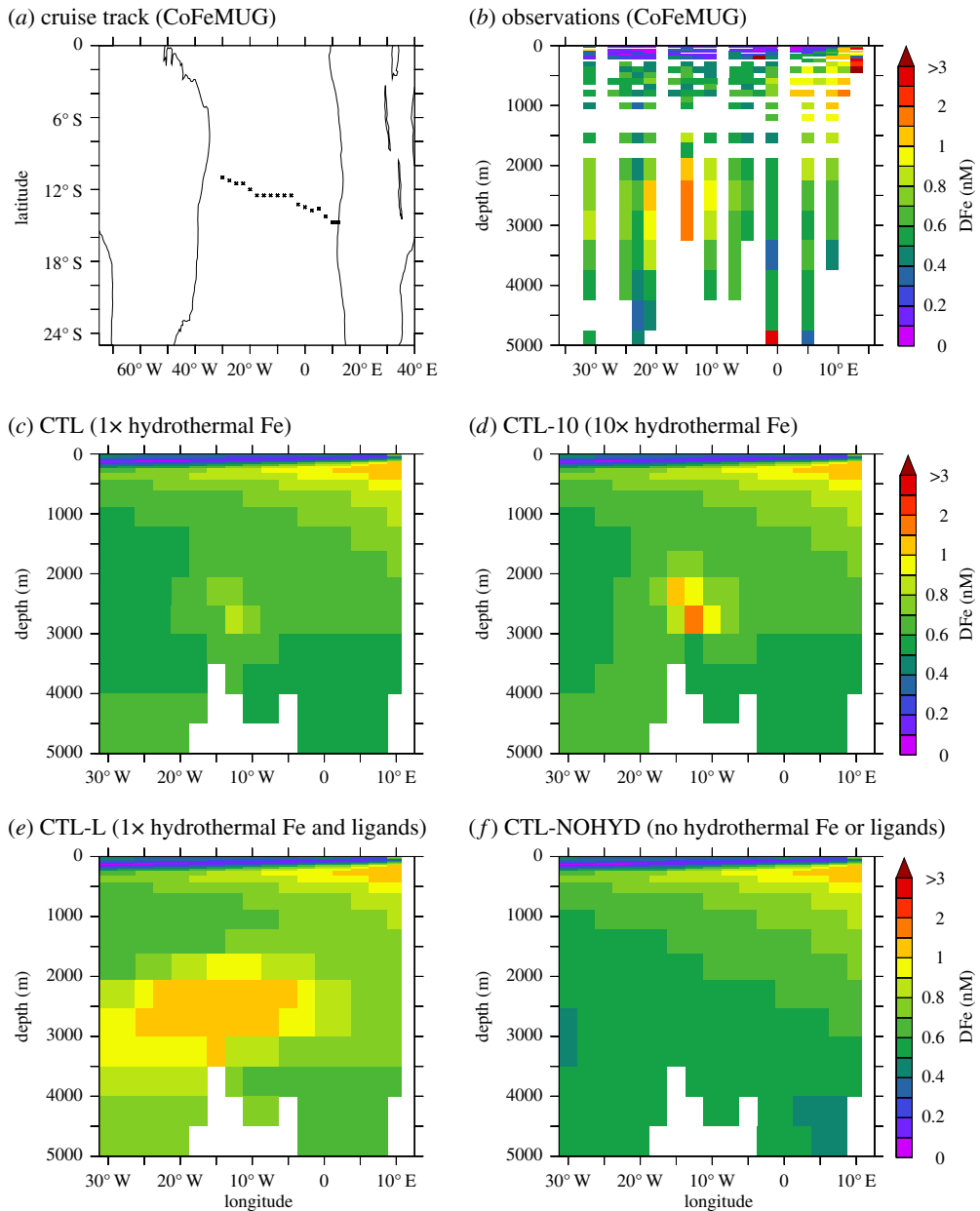


Figure 4. CoFeMUG (a) cruise track and (b) dissolved iron measurements, compared to model output from (c) CTL (hydrothermal iron supply only), (d) CTL-10 (10 times greater hydrothermal iron supply), (e) CTL-L (hydrothermal iron supply alongside an equimolar flux of iron-binding ligands) and (f) CTL-NOHYD (no hydrothermal iron supply).

inter-basin distinctions in the potential density (σ_0) layer where hydrothermal Fe is supplied between the Atlantic, Pacific, Indian and Southern ridges (figure 7a). When we focus on ridges between 1000 and 4000 m (figure 7b), we find hydrothermal Fe is supplied to relatively heavy potential density surfaces by Atlantic ridges ($\sigma_0 = 27.84 \pm 0.04$) and lighter surfaces by Pacific ridges ($\sigma_0 = 27.71 \pm 0.09$) with Indian ($\sigma_0 = 27.76 \pm 0.07$) and Southern ($\sigma_0 = 27.78 \pm 0.07$) ridges falling in between.

When the isopycnal layer to which hydrothermal Fe is supplied is combined with the average σ_0 of the upper Southern Ocean in our physical model (figure 7c), we can compute the potential

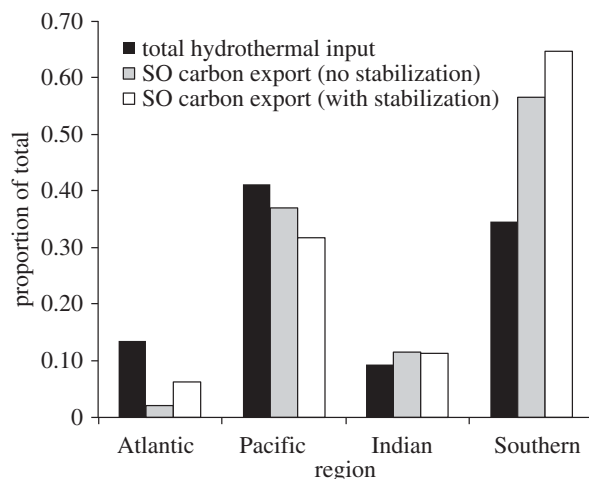


Figure 5. The proportional contribution of ridges in the Atlantic, Pacific and Indian oceans north of 40° S and the Southern Ocean (defined as south of 40° S) to hydrothermal iron input (black bars) and their relative contribution to the effect of hydrothermal iron on Southern Ocean export production without (grey bars, compared to the CTL simulation) and with (white bars, compared to the CTL-L simulation) stabilization by iron-binding ligands. For the grey and white bars, the total effect of hydrothermal iron is first computed by comparing CTL with CTL-NOHYD, then the proportional effect of each ridge system is computed by relating this to the ridge-specific result (i.e. for the Atlantic ridges, dividing the difference between carbon export in ATL and CTL-NOHYD by the difference between CTL and CTL-NOHYD).

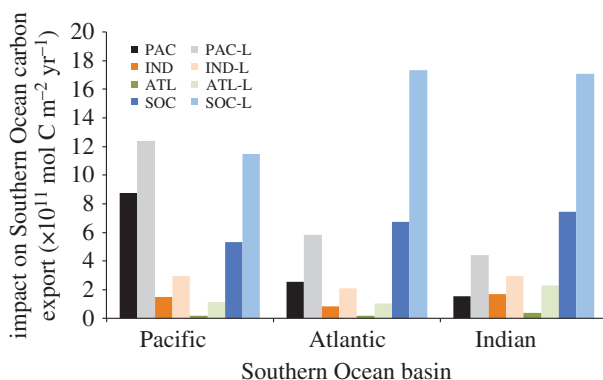


Figure 6. The absolute impact of hydrothermal iron input from different ridge systems in different basins of the Southern Ocean, with and without stabilization by iron-binding ligands (i.e. for the Atlantic, computing the absolute difference in carbon export between ATL and CTL-NOHYD in different geographical sectors of the Southern Ocean).

Table 2. The absolute contribution of specific ridge systems in the Atlantic, Pacific, Indian and Southern regions to overall Southern Ocean carbon export and the sector-specific response; the range reflects the impact without and with hydrothermal iron stabilization.

ridge system	impact on Southern Ocean carbon export ($\times 10^{11}$ mol C yr^{-1})			
	total	Atlantic sector	Pacific sector	Indian sector
Atlantic	0.7–4.4	0.2–1.1	0.2–1.1	0.4–2.3
Pacific	12.8–22.6	2.6–5.9	8.7–12.4	1.5–4.4
Indian	4.0–8.0	0.8–2.1	1.5–3.0	1.7–3.0
Southern	19.5–45.9	6.7–17.3	5.3–11.5	7.4–17.1

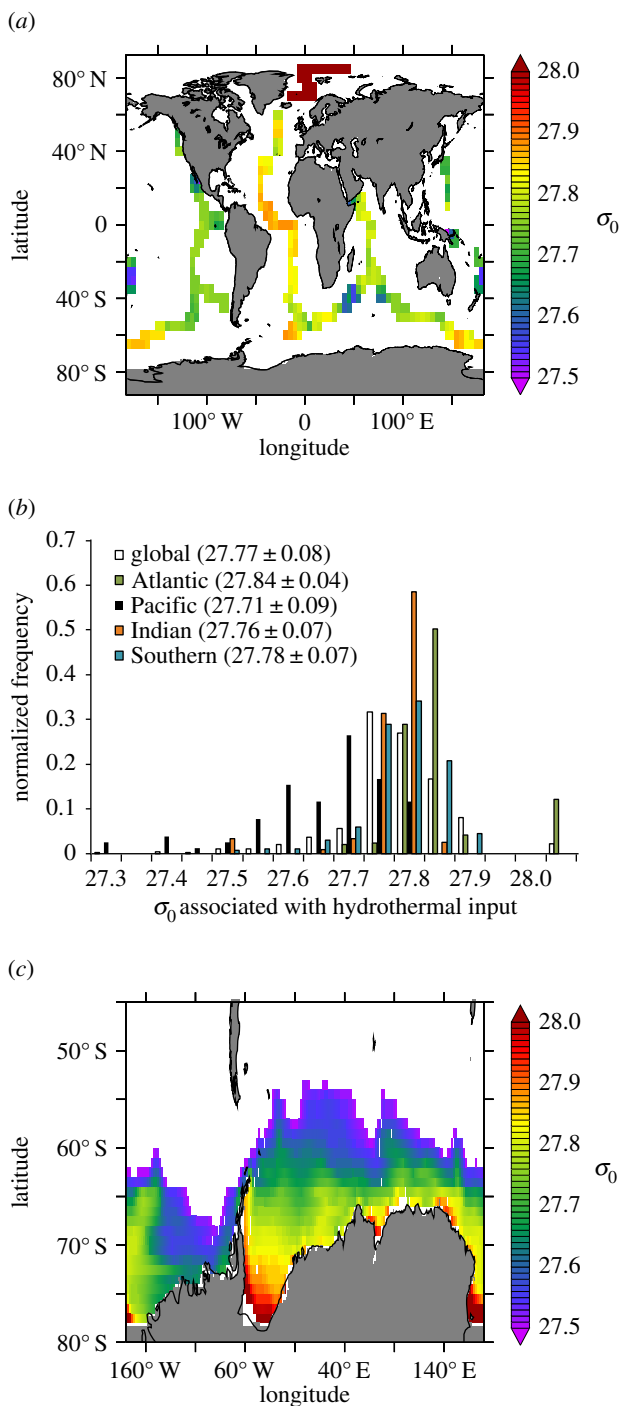


Figure 7. (a) The σ_0 value at the point in the model where hydrothermal iron is input (between 1000 and 4000 m, gridded at 5° horizontal resolution to aid visualization). (b) A histogram of the results from panel (a), focusing on regions south of 60° N. (c) The average value of σ_0 in the model in the upper 100 m in the Southern Ocean.

area of the Southern Ocean impacted by hydrothermal supply from different ridge systems. Owing to their supply of Fe to relatively heavy isopycnal surfaces, Atlantic ridges only influence $7 \times 10^{11} \text{ m}^2$. Alternatively, Pacific ridges influence $50 \times 10^{11} \text{ m}^2$, with Southern and Indian ridges affecting $25 \times 10^{11} \text{ m}^2$ and $17 \times 10^{11} \text{ m}^2$, respectively. In other words, Pacific ridges have a

potentially sevenfold greater influence than Atlantic ridges. We note that this is the maximum possible area over which we might anticipate carbon export to be affected. What is not accounted for is the transit time, which will be important due to the loss of Fe via scavenging, colloidal pumping etc. This explains why there is not a direct connection between these areal extents and the relative carbon export affected by each ridge system (figure 5). For example, the greater impact of Pacific ridges relative to Atlantic ridges in terms of carbon export can be linked to the fact that hydrothermal Fe originated from Atlantic ridges can only reach a small surface area of the Southern Ocean. On the other hand, Southern ridges have a greater carbon export impact than might be expected from the outcrop area of the hydrothermal Fe they supply due to the shorter transit times to Southern Ocean surface waters, which results in reduced Fe losses.

4. Discussion

(a) Evidence of the stabilization of hydrothermal Fe from GEOTRACES sections

Across our modelling experiments, we find some support for the role of Fe stabilization in hydrothermal plumes. The models with stabilization do a much better job for the GP-16 and GA-02 sections, perform similarly to those with greater absolute Fe fluxes for GA-03 and overestimate the hydrothermal anomaly for the CoFeMUG section. This suggests the need for an improved process-level understanding of biogeochemical processes occurring at different ridge crests and within their associated plumes; this includes understanding the nature, abundance and ultimate impact of Fe stabilization. Taken at face value, stabilization of Fe within plumes appears less important for the Atlantic sections, but this may rather reflect the fact that there is at present no study mapping the extent of hydrothermal plumes in the Atlantic Ocean (as has been done in the Pacific). Indeed, the distal signal of hydrothermal Fe seen in the GA-02 transect that occurred away from any known ridge site does require stabilization for our model to be able to reproduce it. On the other hand, the CoFeMUG and GA-03 sections were zonal and sampled across both the ridge crest and the prevailing meridional transport.

At present, there are three working hypotheses for chemical processes governing the longevity of Fe in hydrothermal plumes [33]. The first emphasizes stabilization of Fe by organic ligands [15,34], the second highlights an important role of Fe-sulfur nanoparticle pyrite [35,36], while a third emphasizes the importance of colloidal Fe(III)-oxyhydroxide phases. Each mechanism will have distinct influences on the residence time and reactivity of Fe within the plume. Laboratory studies on synthesized pyrite have documented relatively slow Fe(II)-S₂ oxidation rates which may enhance long range transport [37]. Moreover, the role of nano-pyrite may not be well documented because in filtered samples acidified with hydrochloric acid (as is typical for trace metal sampling), colloidal Fe(II)-S₂ may not oxidize significantly and this Fe therefore may not be detected by analytical techniques employed for the different sections discussed here. Additionally, there is a lack of detailed information on the organic iron-binding ligands in hydrothermal fluids and plumes and, in particular, whether they are functionally distinct from those that make up the wider ocean Fe-binding ligand pool. Finally, colloidal Fe(III)-oxyhydroxides may represent 30–91% of the dissolved Fe pool [38] and their formation and lifetime probably depends on the abundance of particles in the plume. It should be noted that, all things being equal, each process could act in an interconnected manner. For instance, when colloidal Fe(III)-oxyhydroxides dissolve they may be complexed by organic ligands. Similarly, as the Fe(II)-S₂ is slowly oxidized, the produced Fe(III) can form oxyhydroxides or be organically complexed. The prevalence of these potential stabilizing mechanisms is likely to vary between different hydrothermal sites, even within one ridge system. For example, for the well-studied MAR, there is a strong distinction in the sulfide concentrations between the high sulfide system of the TAG site when compared with the low sulfide Rainbow vent sites [39]. Wider afield, Fe(II) was a notable component of the plume signal at TAG [40], but not for the southern East Pacific Rise [24]. Understanding the drivers of these inter-site variations and how they impact on the Fe cycle is a priority.

Generally, high-temperature focused hydrothermal sources are considered when the hydrothermal flux of dissolved Fe into the ocean is examined. However, lower temperature, potentially diffuse sources also play an important role as Fe sources. There are several important factors affecting the relative importance of high-versus low-temperature flow to hydrothermal Fe fluxes. While high-temperature sites release very large amounts of Fe, they also produce copious amounts of particles, which scavenge dissolved Fe in an auto-catalytic manner. Additionally, high-temperature vents are thought to contain little if any metal binding ligands [15], with relatively low concentrations documented [41]. By comparison, lower temperature, often diffuse, sites that surround high-temperature sources have much higher ligand concentrations [41], which can then be entrained into the broader scale plume [15]. Another consideration is that fluids from lower temperature sources have lower Fe concentrations, resulting in a lower abundance of particles. As a result, the lower overall Fe concentrations and lesser scavenging may allow both Fe-colloid and Fe-ligand complex formation to occur within the plume. Recent work suggests that low-temperature sites are more prevalent than previously thought, present both near to and distal from high-temperature sources [42]. These remote sites can thus be additional sources of both Fe and ligands that are vented into a low particle environment, thereby enhancing stabilization through the formation of both Fe-ligand complexes and/or nanoparticle Fe(III)-oxyhydroxides (colloids).

(b) Relative importance of different ridge systems

Overall, Southern ridges are responsible for 57–65% of the total response of the Southern Ocean carbon cycle, with Pacific ridges contributing 32–37% (depending on whether plume stabilization is included or not). Indian ridges and Atlantic ridges are only responsible for 9–12% and 2–6%, respectively. We emphasize that, while the addition of Fe stabilization increases total carbon export (table 2), it only slightly modifies the relative regional breakdown. Overall, our results point to a key importance of ridges located south of 40°S in driving the carbon cycle impact of hydrothermal Fe. However, as yet, there have been relatively few discoveries of hydrothermal ridges along the circum-Antarctic ridge system (but see [43]) in the inter-ridge database [44]. Indeed, a synthesis study suggests a significant number of ridge systems remain to be discovered in the Southern Ocean, pointing out that only eight sites have been recorded along the approximately 20 000 km ridge system around Antarctica [45]. Apart from one study near the Bouvet Triple junction [17], much of our understanding of the broader biogeochemical impacts of hydrothermal vents on the ocean Fe cycle comes from studies that have taken place in the Atlantic [20,21], Pacific [24] and Indian [46] Oceans. As discussed in §4a, it is important to consider how generalized these inferences are for ridges in the Southern Ocean, which we have demonstrated to be the main driver of the carbon cycle response.

Our examination of how hydrothermal Fe affects carbon export in a ventilation framework can be useful to contextualize how observations in the ocean interior may be connected to the surface ocean response. This implies that even if slow spreading ridges on the MAR are supplying more Fe than would be expected from the input of ^3He , this will only influence a relatively small region of the Southern Ocean as Fe is being supplied onto relatively heavy isopycnal surfaces with a small outcrop area. On the other hand, hydrothermal Fe originating from Pacific Ocean ridges has the greatest potential impact due to its supply onto relatively light isopycnal surfaces with a larger Southern Ocean outcrop area. Another important consideration in this regard are the greater oxygen and pH levels in the Atlantic versus the Pacific Ocean. This is important, as it will modify the oxidation rate of Fe, which will then affect its retention in dissolved forms. For example, half lives of Fe(II) range between 17 min at Atlantic hydrothermal sites and 6 h at Pacific sites [47]. Thus, the combination of relatively faster oxidation kinetics that reduce the lifetime of hydrothermal Fe and the relatively small outcrop area due to the flux onto relatively heavy isopycnal surfaces implies a muted carbon cycle influence of Atlantic Ocean hydrothermalism.

5. Synthesis

Much progress has been made on understanding how hydrothermalism affects the ocean iron cycle in recent years, with implications for the global carbon cycle via iron regulation of Southern Ocean export production. The stage is now set for innovative multi-disciplinary studies to address the uncertainties that have been identified via distinct, but complementary studies and tools. We propose that tractable progress can be made by identifying the key questions at a range of scales. First, at the scale of individual vent systems, we need to better understand what sets the end member signals of Fe and ^3He (which is still an excellent conservative tracer in this context) at different vent sites. Second, in the buoyant plume we need to appraise what sets the plume characteristics at local scales, e.g. presence of sulfur, organic ligands, Fe colloids and nanoparticles. Third, at the scale of ridge crest segments we need to understand the distribution of different venting styles, i.e. diffuse versus focused and high versus low temperature, and their relative importance in driving Fe stabilization and transport away from its source. Fourth, in the non-buoyant and dispersing plume, we would benefit from a better understanding of what sets the residence time of the different forms of Fe at the 100–1000 km scale, e.g. degree and manner of stabilization, redox kinetics and soluble–colloidal interactions. Finally, at basin scales, the surface ventilation pathways for Fe supplied onto different isopycnal surfaces and the associated transit times, iron cycling processes and degree of Fe fallout should be considered more deeply. As discussed above, it is likely that the nature of the processes that dominate at these different scales will vary between different vent sites (e.g. high and low sulfur systems), ocean basins (e.g. high and low oxygen levels in the Atlantic and Pacific) and for high-temperature and lower temperature diffuse flow systems. Linking the new ocean section data from GEOTRACES with long-standing knowledge of ocean physical pathways and the on-going detailed work by the hydrothermal community would potentially be transformative.

6. Conclusion

In conclusion, we used a set of model experiments and newly available GEOTRACES datasets to explore the importance of the gross hydrothermal flux and the stabilization of hydrothermal Fe in governing the observed hydrothermal Fe distributions. Overall, we found that in some ocean sections stabilization was important but in others gross fluxes appeared to play a stronger role. In general, we need a better understanding of plume chemistry and how it varies between both different hydrothermal sites and between high-temperature and lower temperature fluxes at a given site. We also examined the role of different ridge systems in regulating carbon export in the Southern Ocean. Overall, Southern ridges were found to be dominant, followed by Pacific ridges, with Indian and then Atlantic ridges playing a muted role. Southern ridge systems are relatively poorly explored and future exploration will be invaluable in better representing their effect. We highlight strong inter-basin differences in the isopycnal layer onto which hydrothermal Fe is supplied between the Atlantic and Pacific basins, which affects the area of the Southern Ocean that may be influenced. When linked to the relatively faster oxidation kinetics in the Atlantic Ocean, this suggests a small influence of Atlantic ridges on Southern Ocean carbon cycling. Overall, we present a new synthesis of scales, within which further observational and modelling work, bridging across disciplines, may make future progress in better constraining the influence of hydrothermal Fe supply on the biogeochemical cycling of the oceans.

Data accessibility. Model data are available by contacting A.T.

Authors' contributions. A.T. and J.R. designed the study, discussed the results and co-wrote the paper. A.T. carried out the model experiments and their analysis. Both authors gave final approval for publication.

Competing interests. The authors declare that there are no competing interests.

Funding. All model simulations made use of the facilities of N8 HPC Centre of Excellence, provided and funded by the N8 consortium and EPSRC (grant no. EP/K000225/1). The Centre is coordinated by the

Universities of Leeds and Manchester. J.R. is partially funded by NSF-OCE 1237011 and UW-JISAO under NOAA Cooperative Agreement NA15OAR4320063 (2015–2020).

Acknowledgements. We thank the participants of the Royal Society discussion meeting ‘Biological and climatic impacts of ocean trace element chemistry’ for their input. Three anonymous reviewers provided valuable constructive comments that improved the final manuscript. This is JISAO contribution number 2609 and PMEL number 4452.

References

1. Volk T, Hoffert MI. 1985 Ocean carbon pumps: analysis of relative strengths and efficiencies in ocean-driven atmospheric CO₂ changes. *The carbon cycle and atmospheric CO₂: natural variations archean to present* (eds ET Sundquist, WS Broecker), pp. 99–110. Washington, DC: American Geophysical Union. (doi:10.1029/GM032p0099)
2. Sarmiento JL, Orr JC. 1991 Three-dimensional simulations of the impact of Southern Ocean nutrient depletion on atmospheric CO₂ and ocean chemistry. *Limnol. Oceanogr.* **36**, 1928–1950. (doi:10.4319/lo.1991.36.8.1928)
3. Landing WM, Bruland KW. 1987 The contrasting biogeochemistry of iron and manganese in the Pacific Ocean. *Geochim. Cosmochim. Acta* **51**, 29–43. (doi:10.1016/0016-7037(87)90004-4)
4. Martin JH, Gordon RM, Fitzwater SE. 1990 Iron in Antarctic waters. *Nature* **345**, 156–158. (doi:10.1038/345156a0)
5. Gordon RM, Martin JH, Knauer GA. 1982 Iron in northeast Pacific waters. *Nature* **299**, 611–612. (doi:10.1038/299611a0)
6. Boyd PW *et al.* 2007 Mesoscale iron enrichment experiments 1993–2005: synthesis and future directions. *Science* **315**, 612–617. (doi:10.1126/Science.1131669)
7. de Baar HJW *et al.* 2005 Synthesis of iron fertilization experiments: from the Iron Age in the Age of Enlightenment. *J. Geophys. Res.* **110**, C09516. (doi:10.1029/2004jc002601)
8. Moore CM *et al.* 2013 Processes and patterns of oceanic nutrient limitation. *Nat. Geosci.* **6**, 701–710. (doi:10.1038/ngeo1765)
9. Jickells TD *et al.* 2005 Global iron connections between desert dust, ocean biogeochemistry, and climate. *Science* **308**, 67–71. (doi:10.1126/Science.1105959)
10. Martinez-Garcia A, Sigman DM, Ren H, Anderson RF, Straub M, Hodell DA, Jaccard SL, Eglinton TI, Haug GH. 2014 Iron fertilization of the Subantarctic ocean during the last ice age. *Science* **343**, 1347–1350. (doi:10.1126/science.1246848)
11. Edmond JM, Measures C, McDuff RE, Chan LH, Collier R, Grant B, Gordon LI, Corliss JB. 1979 Ridge crest hydrothermal activity and the balances of the major and minor elements in the ocean: the Galapagos data. *Earth Planet. Sci. Lett.* **46**, 1–18. (doi:10.1016/0012-821x(79)90061-x)
12. German CR, Seyfried WE. 2014 Hydrothermal processes. *Treatise Geochem.* 191–233. (doi:10.1016/b978-0-08-095975-7.00607-0)
13. Elderfield H, Schultz A. 1996 Mid-ocean ridge hydrothermal fluxes and the chemical composition of the ocean. *Annu. Rev. Earth Planet. Sci. Lett.* **24**, 191–224. (doi:10.1146/annurev.earth.24.1.191)
14. de Baar HJ, de Jong JT. 2001 Distributions, sources and sinks of iron in seawater. In *The biogeochemistry of iron in seawater* (eds DR Turner, KA Hunter), pp. 123–254. Chichester, UK: Wiley.
15. Bennett SA, Achterberg EP, Connelly DP, Statham PJ, Fones GR, German CR. 2008 The distribution and stabilisation of dissolved Fe in deep-sea hydrothermal plumes. *Earth Planet. Sci. Lett.* **270**, 157–167. (doi:10.1016/j.epsl.2008.01.048)
16. Boyle EA, Bergquist BA, Kayser RA, Mahowald N. 2005 Iron, manganese, and lead at Hawaii Ocean Time-series station ALOHA: temporal variability and an intermediate water hydrothermal plume. *Geochim. Cosmochim. Acta* **69**, 933–952. (doi:10.1016/j.gca.2004.07.034)
17. Klunder MB, Laan P, Middag R, De Baar HJW, van Ooijen JC. 2011 Dissolved iron in the Southern Ocean (Atlantic sector). *Deep Sea Res. Part II: Top. Stud. Oceanogr.* **58**, 2678–2694. (doi:10.1016/j.dsr2.2010.10.042)
18. Klunder MB, Bauch D, Laan P, de Baar HJW, van Heuven S, Ober S. 2012 Dissolved iron in the Arctic shelf seas and surface waters of the central Arctic Ocean: impact of Arctic river water and ice-melt. *J. Geophys. Res. Oceans* **117**, C01027. (doi:10.1029/2011jc007133)

19. Tagliabue A *et al.* 2010 Hydrothermal contribution to the oceanic dissolved iron inventory. *Nat. Geosci.* **3**, 252–256. (doi:10.1038/ngeo818)
20. Hatta M, Measures CI, Wu J, Roshan S, Fitzsimmons JN, Sedwick P, Morton P. 2015 An overview of dissolved Fe and Mn distributions during the 2010–2011 U.S. GEOTRACES north Atlantic cruises: GEOTRACES GA03. *Deep Sea Res. Part II: Top. Stud. Oceanogr.* **116**, 117–129. (doi:10.1016/j.dsr2.2014.07.005)
21. Saito MA, Noble AE, Tagliabue A, Goepfert TJ, Lamborg CH, Jenkins WJ. 2013 Slow-spreading submarine ridges in the South Atlantic as a significant oceanic iron source. *Nat. Geosci.* **6**, 775–779. (doi:10.1038/Ngeo1893)
22. Wu J, Wells ML, Rember R. 2011 Dissolved iron anomaly in the deep tropical–subtropical Pacific: evidence for long-range transport of hydrothermal iron. *Geochim. Cosmochim. Acta* **75**, 460–468. (doi:10.1016/j.gca.2010.10.024)
23. Fitzsimmons JN, Boyle EA, Jenkins WJ. 2014 Distal transport of dissolved hydrothermal iron in the deep South Pacific Ocean. *Proc. Natl Acad. Sci. USA* **111**, 16 654–16 661. (doi:10.1073/pnas.1418778111)
24. Resing JA, Sedwick PN, German CR, Jenkins WJ, Moffett JW, Sohst BM, Tagliabue A. 2015 Basin-scale transport of hydrothermal dissolved metals across the South Pacific Ocean. *Nature* **523**, 200–203. (doi:10.1038/nature14577)
25. Aumont O, Ethé C, Tagliabue A, Bopp L, Gehlen M. 2015 PISCES-v2: an ocean biogeochemical model for carbon and ecosystem studies. *Geosci. Model Dev.* **8**, 2465–2513. (doi:10.5194/gmd-8-2465-2015)
26. Tagliabue A *et al.* 2016 How well do global ocean biogeochemistry models simulate dissolved iron distributions? *Glob. Biogeochem. Cycles* **30**, 149–174. (doi:10.1002/2015gb005289)
27. Völker C, Tagliabue A. 2015 Modeling organic iron-binding ligands in a three-dimensional biogeochemical ocean model. *Mar. Chem.* **173**, 67–77. (doi:10.1016/j.marchem.2014.11.008)
28. Rijkenberg MJ, Middag R, Laan P, Gerringa LJ, van Aken HM, Schoemann V, de Jong JT, de Baar HJ. 2014 The distribution of dissolved iron in the West Atlantic Ocean. *PLoS ONE* **9**, e101323. (doi:10.1371/journal.pone.0101323)
29. Tagliabue A, Aumont O, Bopp L. 2014 The impact of different external sources of iron on the global carbon cycle. *Geophys. Res. Lett.* **41**, 920–926. (doi:10.1002/2013gl059059)
30. Laws EA, Falkowski PG, Smith WO, Ducklow H, McCarthy JJ. 2000 Temperature effects on export production in the open ocean. *Glob. Biogeochem. Cycles* **14**, 1231–1246. (doi:10.1029/1999gb001229)
31. Schlitzer R. 2002 Carbon export fluxes in the Southern Ocean: results from inverse modeling and comparison with satellite-based estimates. *Deep Sea Res. Part II: Top. Stud. Oceanogr.* **49**, 1623–1644. (doi:10.1016/s0967-0645(02)00004-8)
32. Henson SA, Sanders R, Madsen E, Morris PJ, Le Moigne F, Quartly GD. 2011 A reduced estimate of the strength of the ocean’s biological carbon pump. *Geophys. Res. Lett.* **38**, L04606. (doi:10.1029/2011gl046735)
33. Tagliabue A. 2014 More to hydrothermal iron input than meets the eye. *Proc. Natl Acad. Sci. USA* **111**, 16 641–16 642. (doi:10.1073/pnas.1419829111)
34. Toner BM, Fakra SC, Manganini SJ, Santelli CM, Marcus MA, Moffett JW, Rouxel O, German CR, Edwards KJ. 2009 Preservation of iron(II) by carbon-rich matrices in a hydrothermal plume. *Nat. Geosci.* **2**, 197–201. (doi:10.1038/ngeo433)
35. Yücel M, Gartman A, Chan CS, Luther GW. 2011 Hydrothermal vents as a kinetically stable source of iron-sulphide-bearing nanoparticles to the ocean. *Nat. Geosci.* **4**, 367–371. (doi:10.1038/ngeo1148)
36. Gartman A, Findlay AJ, Luther GW. 2014 Nanoparticulate pyrite and other nanoparticles are a widespread component of hydrothermal vent black smoker emissions. *Chem. Geol.* **366**, 32–41. (doi:10.1016/j.chemgeo.2013.12.013)
37. Gartman A, Luther GW. 2014 Oxidation of synthesized sub-micron pyrite (FeS₂) in seawater. *Geochim. Cosmochim. Acta* **144**, 96–108. (doi:10.1016/j.gca.2014.08.022)
38. Gledhill M, Buck KN. 2012 The organic complexation of iron in the marine environment: a review. *Front. Microbiol.* **3**, 69. (doi:10.3389/fmicb.2012.00069)
39. Findlay AJ, Gartman A, Shaw TJ, Luther GW. 2015 Trace metal concentration and partitioning in the first 1.5 m of hydrothermal vent plumes along the Mid-Atlantic Ridge: TAG, Snakepit, and Rainbow. *Chem. Geol.* **412**, 117–131. (doi:10.1016/j.chemgeo.2015.07.021)

40. Sedwick PN, Sohst BM, Ussher SJ, Bowie AR. 2015 A zonal picture of the water column distribution of dissolved iron(II) during the U.S. GEOTRACES North Atlantic transect cruises. *Deep Sea Res. Part II: Top. Stud. Oceanogr.* **116**, 166–175. (doi:10.1016/j.dsr2.2014.11.004)
41. Sander SG, Koschinsky A, Massoth G, Stott M, Hunter KA. 2007 Organic complexation of copper in deep-sea hydrothermal vent systems. *Environ. Chem.* **4**, 81–89. (doi:10.1071/en06086)
42. Baker ET, Resing JA, Haymon RM, Tunnicliffe V, Lavelle JW, Martinez F, Ferrini V, Walker SL, Nakamura K. 2016 How many vent fields? New estimates of vent field populations on ocean ridges from precise mapping of hydrothermal discharge locations. *Earth Planet. Sci. Lett.* **449**, 186–196. (doi:10.1016/j.epsl.2016.05.031)
43. Hahm D, Baker ET, Siek Rhee T, Won Y-J, Resing JA, Lupton JE, Lee W-K, Kim M, Park S-H. 2015 First hydrothermal discoveries on the Australian-Antarctic Ridge: discharge sites, plume chemistry, and vent organisms. *Geochem. Geophys. Geosyst.* **16**, 3061–3075. (doi:10.1002/2015gc005926)
44. Beaulieu SE, Baker ET, German CR, Maffei A. 2013 An authoritative global database for active submarine hydrothermal vent fields. *Geochem. Geophys. Geosyst.* **14**, 4892–4905. (doi:10.1002/2013gc004998)
45. Beaulieu SE, Baker ET, German CR. 2015 Where are the undiscovered hydrothermal vents on oceanic spreading ridges? *Deep Sea Res. Part II: Top. Stud. Oceanogr.* **121**, 202–212. (doi:10.1016/j.dsr2.2015.05.001)
46. Nishioka J, Obata H, Tsumune D. 2013 Evidence of an extensive spread of hydrothermal dissolved iron in the Indian Ocean. *Earth Planet. Sci. Lett.* **361**, 26–33. (doi:10.1016/j.epsl.2012.11.040)
47. Field MP, Sherrell RM. 2000 Dissolved and particulate Fe in a hydrothermal plume at 9°45'N, East Pacific Rise. *Geochim. Cosmochim. Acta* **64**, 619–628. (doi:10.1016/s0016-7037(99)00333-6)